Penning Ionization in Optical Collisions

G. Woestenenk, P. van der Straten, and A. Niehaus
Debye Institute, Department of Atomic- and Interface Physics - Utrecht University
P. O. Box 80.000, 3508 TA Utrecht, The Netherlands
(submitted to Phys. Rev. A)

We have studied binary collisions of cold He (2^3S_1) atoms under the influence of nearly-resonant light. The light is tuned below the atomic $2^3S_1 \rightarrow 2^3P_2$ transition. A semi-classical model is developed, calculating the absolute ionization rate as a function of the detuning of the light. The calculated ionization rate is compared with measurements and with values that have appeared in the literature. Good agreement is found between theory and measurements.

I. INTRODUCTION

Since the development of laser cooling and trapping [1], cold atoms are widely studied. Most experiments studying cold atoms are performed in a magneto-optical trap (MOT). The use of MOT's triggered the interest in optical collisions, which are binary collisions in the presence of nearly resonant light. The colliding atoms are excited to an attractive excited state potential. The reason for the interest in these collisions is that they are important channels for trap loss in MOT's.

The first studies of collisions of cold atoms in the presence of nearly resonant light have been done with alkali-atoms. In alkali-atom traps we can distinguish three mechanisms involving optical collisions which lead to trap loss [2] (meer referenties?). In the radiative escape mechanism (RE) the colliding atoms are accelerated on the attractive potential. If the kinetic energy, that is gained by the atoms when spontaneously decaying back to the ground state, is large enough they can escape the trap. In a fine-structure changing collision (FS) the population can be transferred to a different fine-structure state when the atoms are accelerated towards each other. In that case the atoms gain the energy difference between the fine-structure states and can escape the trap. Furthermore in the last mechanism a hyperfine-structure changing collision (HFS) can take place where the hyperfine state of the ground state can be changed. All of the three above mechanisms have been studied in alkali-atom traps by measuring trap loss.

Optical collisions of cold metastable rare gas atoms cannot only be studied with trap loss measurements, but also by measuring ionization rates. In a close collision of two metastable He atoms the probability for Penning ionization or associative ionization is almost unity for singlet and triplet states and spin forbidden for quintet states [15]. An experiment where the ionization rate is measured is a method to detect an optical collision with almost zero background. This is a great advantage above trap loss measurements. Optical collisions of cold Xe* atoms have been successfully studied by measuring ions [3], where the ion rate induced by nearly resonant laser light was measured as a function of the detuning of the light. A similar experiment has been carried out for He* [4]. Furthermore, in the literature have appeared various values for loss rates and ionization rates for He (2^3S_1 - 2^3P_2) collisions [4–8]. These rates disagree with each other by factors 2 to 100. In this work we present new measurements of the ionization rate for cold he (2^3S_1 - 2^3P_2) collisions. The results are compared with the results that have appeared in the literature by giving a consistent definition of the ionization rate.

Optical collisions have also been studied theoretically. For the general case of one molecular ground and one molecular excited state models have been developed which provide a qualitative description of the increase of the collision rate constant in the presence of nearly-resonant light [9–11]. The Julienne-Vigué model [10] gives a rather accurate quantum mechanical description. To obtain more insight in the relevant processes we have developed a semi-classical version of such a two-state model. A first version of the model has already been presented [4,12]. In this work we present a corrected and improved version of the model, in which we use a partial wave formulation and take the finite lifetime of the excited state into account. The model is used to calculate an absolute ionization rate constant, which will be compared with the values that have appeared in the literature.

II. EXPERIMENTAL

The experiments are performed in a magneto-optical trap (MOT). The trap is loaded with a beam of He* atoms produced in a DC-discharge source, which is cooled with liquid helium. The mean velocity of the atoms leaving the source is 300 m/s. Before the He* atoms are trapped in the MOT, they are Zeeman slowed with a counter-propagating laser beam while the required Zeeman shift is produced by the magnetic field of the MOT coils. Typically we trap 10^6 atoms with a temperature of 1 mK and a density of a few times 10^9 cm^{-3}. The atoms are cooled on the $2^3S_1 \rightarrow 2^3P_2$ transition, which has a wavelength of 1083 nm.

A probe laser is scanned in frequency around the 2^3S_1 - 2^3P_2 asymptote and the ion rate is measured as a function of the probe laser frequency. The produced ions are measured with micro-channel plates. The laser light is generated by diode lasers. The frequency of the probe laser light is calibrated using a Fabry-Perot interferometer for the relative frequency scale and the Lamb dip to determine the absolute frequency. The uncertainty in the absolute frequency scale is 20 MHz.

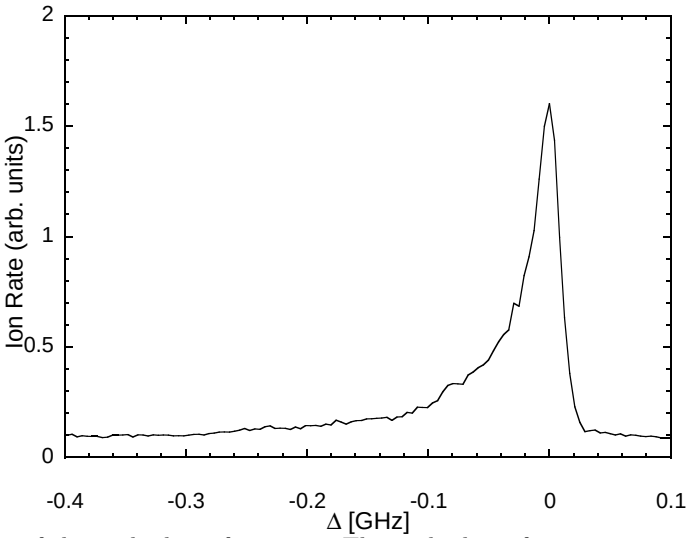

FIG. 1. Ion rate as a function of the probe laser frequency. The probe laser frequency is expressed as the detuning Δ with respect to the 2^3S_1 - 2^3P_2 asymptote. The saturation parameter of the probe laser was $s_0 = 450$.

The trapping laser is periodically switched off, since we are only interested in ionization induced by the probe laser. The laser is switched off for 25% of the period, by detuning its frequency 500 MHz to the red of the $2^3S_1 \rightarrow 2^3P_2$ transition. This is far enough to ensure that the trapping laser does not induce many ions. The period when the trapping laser is switched off is defined as the probing period, while the period when the trapping laser is switched on is defined as the trapping period. The probing period is 20 μs, which is short enough to avoid significant expansion of the cloud of trapped atoms. The probe laser is switched off in the trapping period using an acousto-optical modulator, from which the first order diffraction beam is used as the probe laser. In this way we make sure that the cloud of trapped atoms is not perturbed by the probe laser. The ion signal is gated and can be measured both in the probing period and in the trapping period. In the probing period the detuning-dependent ion rate is measured, while the signal in the trapping period is used to monitor the stability of the trapped cloud. A typical scan time is 100 s. A typical measurement is shown in Fig. 1. Several scans were added to produce the spectrum shown in the figure.

III. THE TWO STATE MODEL

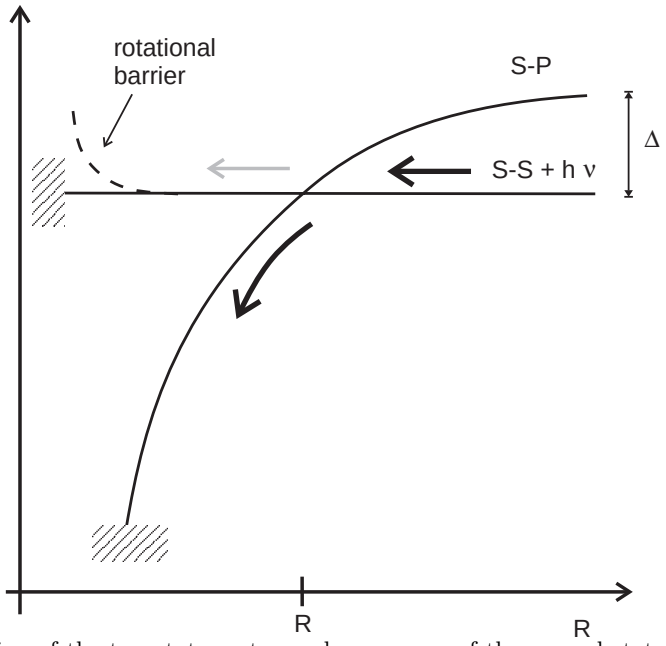

FIG. 2. Schematic representation of the two-state system, where energy of the ground state S-S potential is shifted by the energy of a photon. The light is detuned with Δ to the red of the S-P asymptote. A transition can occur at the crossing at R_c and the grey arrow indicates the population that is not excited. The shaded regions indicate the regions where PI can take place. The potential barrier on the S-S potential (for $\ell \neq 0$) is shown with the dashed line.

In Fig. 2 a schematic representation of the two-state system is shown. The laser light is detuned to the red of the 2^3S_1 - 2^3P_2 asymptote with a detuning Δ. For a large detuning of $\Delta \gg \Gamma$, where Γ is the linewidth of the transition, the excitation can only take place around the Condon point R_c, where a transition can occur without appreciable change of the relative kinetic energy of the atoms.

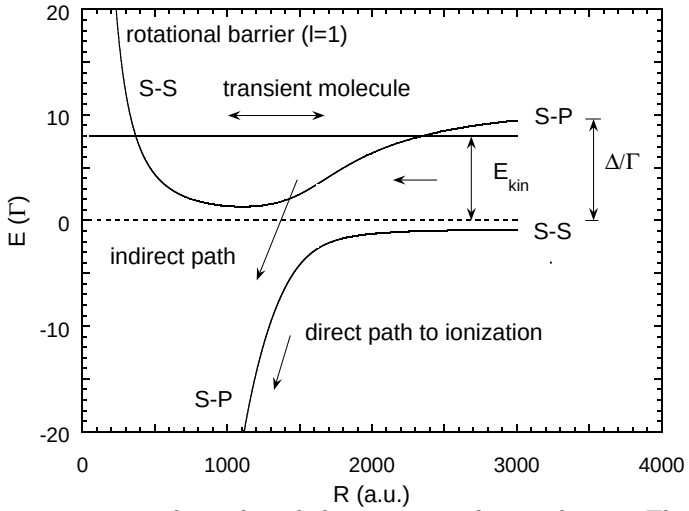

FIG. 3. Molecular dressed state picture, where the adiabatic potentials are shown. The system can ionize directly or indirectly. For $\ell \neq 0$ the rotational barrier on the S-S potential prevents the transient molecule to reach small internuclear distances.

We describe the system in terms of a dressed-state picture to obtain an insightful and quantitative description, where the ground and the excited state potential are coupled by the light field. The electronic coupling is given by

the Rabi frequency Ω, which can be found from the atomic Rabi frequency $\Omega_{at}^2 = s_0/2\Gamma_{at}^2$, and is responsible for an avoided crossing of the adiabatic potentials, which can be seen in Fig. 3. The transition from the ground to the excited state is described in terms of the electronic coupling. Collisions in the ensemble of 2^3S atoms occur on the ground state potential, with velocities determined by the temperature of the MOT. After having passed the region around the Condon distance, a system can be either on the lower adiabatic potential, or on the upper adiabatic potential. Being on the lower one at $R < R_c$ means to be in the excited state. The probability for this is given by the Landau-Zener expression [11]:

$$P = 1 - \exp\left(-\frac{\pi\hbar\Omega^2}{2\alpha v_{rad}}\right), \tag{1}$$

where α is the gradient of the difference between the diabatic potentials at the crossing point R_c, and v_{rad} is the radial velocity. We have used the relation $|H_{12}|^2 = (\Omega/2)^2$ to express the electronic coupling in terms of the Rabi frequency. The detuning Δ is used to determine R_c via the relation $\Delta = C_3/R_c^3$. The Condon distances relevant for the present discussion are found to be in the order of 100 - 1000 atomic units. At these large distances α is given by $\alpha = 3C_3/R_c^4$ and the local Ω is approximately constant and can be calculated from Ω_{at}.

We use Eq. 1 to formulate an expression for the ionization rate constant. The model assumes that close collisions lead to PI with 100% probability, except if this is forbidden by the spin selection rule. This is a valid assumption, which has been verified even for thermal collisions [15]. The expression is given in terms of the partial wave expansion of an inelastic scattering cross section described by O_ℓ, which is the angular momentum dependent ionization probability. The ionization rate constant K depends on the detuning Δ, the laser intensity s_0, and the velocity v, and is written as [10]

$$K(\Delta, s_0, v) = \frac{\pi\hbar^2 v}{\mu^2} \sum_{\ell=0}^{\ell_{max}} (2\ell+1)\Theta_\ell O_\ell, \tag{2}$$

where μ is the reduced mass, and Θ_ℓ is a step function. The step function Θ_ℓ is introduced, because the collision system has a well defined *gerade (g)* or *ungerade (u)* symmetry, which restricts the allowed partial waves. Since the collision system is symmetric the weight of the allowed partial waves is doubled. Thus:

	even ℓ	odd ℓ
gerade ground state:	$\Theta_\ell = 2$	$\Theta_\ell = 0$
ungerade ground state:	$\Theta_\ell = 0$	$\Theta_\ell = 2$

The summation in Eq. 2 has to be carried out until a certain maximum angular momentum ℓ_{max}. The maximum angular momentum is limited by the rotational barrier in the ground state and the kinetic energy of the collision system. The system needs to reach the Condon point R_c in order make the transition, reach small internuclear distances on the excited state potential, and contribute to the ionization. Hence ℓ_{max} is determined by the relation:

$$\frac{\hbar^2}{2\mu}\frac{\ell_{max}(\ell_{max}+1)}{R_c^2} - \frac{C_6}{R_c^6} > \frac{1}{2}\mu v^2. \tag{3}$$

In order to find an expression for O_ℓ, we have to distinguish the different possible paths leading to ionization. Below we make a distinction between direct and indirect paths of ionization, either in the excited state (SP) or in the ground state (SS):

- The direct SP contribution is possible for all allowed values of ℓ. The system is excited on the way in at the avoided crossing, then approaches small distances on the excited state potential without decaying spontaneously by photon emission and Penning ionizes on the excited state potential. The corresponding probability is given by $P_\ell S_\ell$, where P_ℓ is defined in Eq. 1 and $S_\ell = \exp(-\Gamma t_\ell)$ is the survival probability in the excited state during the approach time t_ℓ. This time is obtained from integration along the ℓ-dependent trajectory, using $t_\ell = \int dR/v_\ell(R)$, with $v_\ell(R)$ the ℓ-dependent radial velocity on the excited state potential curve.

- The indirect SP contribution has not been considered in earlier models [4,12]. In this case the system is not excited on the way in. If $\ell \neq 0$ and $E_{kin} < \Delta$, the system is partly captured and forms a transient molecule in the upper adiabatic potential (see Fig. 3). This molecule can either dissociate by diabatic crossing on the way out, or ionize after a diabatic crossing on the way in. While a correct calculation should use amplitudes and phases to calculate this contribution, we content ourselves here with a calculation using probabilities. The

total contribution can then be calculated by summation of the successive contributions, *i.e.*, the contributions after 1,2,3, .. oscillations. The infinite sum can be carried out and leads to the ionization probability $P_\ell S_\ell(1-P_\ell)/(1+P_\ell)$.

- For the direct SS contribution the system is not excited on the way in at the avoided crossing, then approaches small distances on the ground state potential and Penning ionizes on the ground state potential. The corresponding probability is $(1-P_\ell)$. At the low collision energies in the MOT only partial waves with $\ell = 0$ can penetrate the rotational barrier on the ground state and reach the small internuclear distances, where PI occurs, *i.e.* only $\ell = 0$ contributes to the ionization.
- For the indirect SS contribution the system is excited on the way in, then spontaneously decays to the ground state, and Penning ionizes in the ground state, which is only possible for $\ell = 0$. The corresponding probability is $P_\ell(1-S_\ell)$.

The ionization probability to be used in Eq. 2 thus becomes the sum of those four terms:

$$\begin{aligned} O_\ell = &\ P_\ell S_\ell + P_\ell S_\ell\,(1-P_\ell)\,/\,(1+P_\ell) = 2P_\ell S_\ell/\,(1+P_\ell) \quad \text{for } \ell \neq 0 \\ O_\ell = &\ P_\ell S_\ell + (1-P_\ell) + P_\ell(1-S_\ell) \ = 1 \qquad\qquad\qquad\qquad\quad \text{for } \ell = 0. \end{aligned} \tag{4}$$

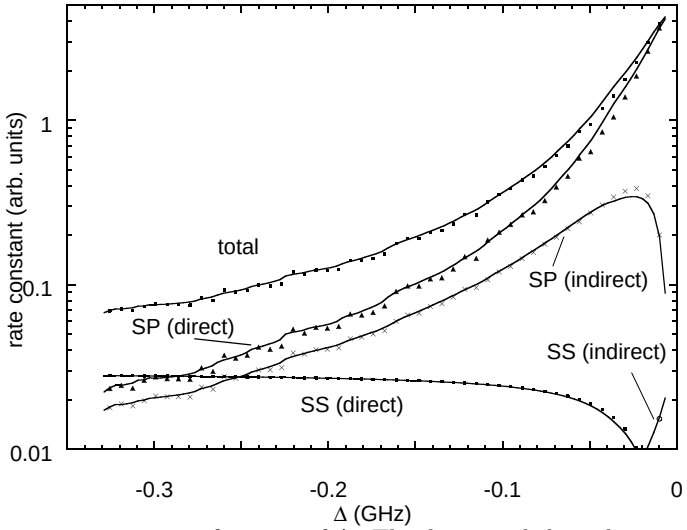

FIG. 4. Calculated ionization rate constant as a function of Δ. The direct and the indirect contributions, as discussed in the text, are shown. The symbols represent the calculation. A smoothed line is drawn to correct for structure that arises, due to the finite steps in the velocity distribution that have been used in the calculation.

In a numerical program, the evaluation of expression Eq. 4 for the ionization rate constant is easily carried out. In Fig. 4 the total calculated ionization rate constant and the direct and indirect contributions to it are shown. It can be seen that the direct SP contribution is the dominant contribution. The crucial quantity that determines the quality of the result is the excitation probability function, which is approximated using the Landau-Zener formula in Eq. 1. While this approximation is expected to be valid for large detunings ($\Delta \gg \Gamma$), when the region of distances where transitions induced by the radiation occur is rather narrow [13], its validity for small detunings is questionable. To check whether the approximation is good enough, we have calculated the excitation probability with a quantum-mechanical model (N.B. eventueel meer hierover op deze plaats) and find the agreement with the semi-classical Landau-Zener excitation probability to be good.

IV. CALCULATION OF THE ABSOLUTE IONIZATION RATE CONSTANT

In this section we describe the procedure we followed to calculate the absolute ionization rate constant for the 2^3S_1 - 2^3P_2 system, using the semi-classical two-state model described above.

To calculate the absolute ionization rate we have used the actual long-range potential curves connected to the 2^3S_1 - 2^3P_2 asymptote. The potentials have been constructed using the Movre-Pichler analysis [14]. This method has

been used to calculate long-range potentials for alkali-atoms and we have applied it to the He 2^3S_1 - 2^3P_2 system. (ref?) In total there are 54 potentials for the He 2^3S_1 - 2^3P system. For the calculation of the ionization rate the nine potentials which are attractive and connect to the 2^3S_1 - 2^3P_2 asymptote are used. These potentials are shown in Fig. ? At the large distances that are relevant for the calculation of the ionization rate constant, the potentials behave as $-C_3/R^3$. Due to the fine-structure interaction the potentials are mixed and hence deviate from the $-C_3/R^3$ behavior at distances of 100 - 500 a_0, while at smaller distances of 20 - 100 a_0 the potentials behave again as $-C_3/R^3$. The potentials have been calculated in the range from 20 - 1000 a_0. (meer?)

For all potentials we have calculated the C_3 coefficients, the linewidths for spontaneous emission Γ, and the Penning ionization probability p. The PI probability is deduced from the spin character of the state at large internuclear distances, where the spin states are mixed. We have assumed that at short range, where S is a good quantum number, the singlet and triplet spin states ionize with unity probability and the quintet states ionize with zero probability. A list of the properties of the potentials connected to the 2^3S_1 - 2^3P_2 asymptote is given in Tab. I.

The excited state potentials can be populated from various potentials connected to the 2^3S_1 - 2^3S_1 potentials. These potentials are degenerate at the distances where the excitations are made, but we characterize them by the total spin quantum number and its projection on the internuclear axis. Since the potentials are degenerate we can choose any axis. We found that when the system is excited to the 2^3S_1 - 2^3P_2 system, every ground state potential is mainly coupled to one excited state potential and that the coupling to other excited states is an order of magnitude weaker. In principle, allowed contributions from all ground to all excited states should be taken into account, but we have used an approximation where only the dominant contribution has been included in the calculation. We find that all dominant transitions are π transitions. For the excited states the spin states are mixed and the Hund's case (a) ground states couple only with a fraction of the excited Hund's case (c) states. This fraction is given by w, where w is the population probability of the fraction of the excited state coupling with the ground state. We use w to obtain the Rabi frequency for each ground to excited state transition, since we need the Rabi frequency to evaluate the Landau-Zener expression. The characteristic Rabi frequency Ω_{mol} for each pair is given by $\Omega_{mol} = (\Omega_{at}/\Gamma_{at})\,\Gamma_{mol}\sqrt{w}$.

TABLE I. Properties of the excited state potentials connected to the 2^3S_1 - 2^3P_1 asymptote. The C_3 coefficient is expressed in terms of the dispersion coefficient μ (iets hierover?). The excited fraction is the fraction of the state that can be excited from the ground state. The polarization is the polarization of the light required to make the excitation. The ground state potentials where they are excited from are also shown.

Ground state		Excited state					
Symm.	Σ	Symm.	Γ (Γ_{at})	C_3 (μ)	w	p	pol.
$^1\Sigma_g^+$	0	0_u^+	1.271	-0.536	0.509	0.89	π
$^5\Sigma_g^+$	-2	2_u	1.016	-0.455	0.394	0.59	π
$^5\Sigma_g^+$	-1	1_u	1.582	-0.313	0.522	0.27	π
$^5\Sigma_g^+$	0	0_u^+	1.984	-0.242	0.505	0.08	π
$^5\Sigma_g^+$	1	1_u	1.582	-0.313	0.522	0.275	π
$^5\Sigma_g^+$	2	2_u	1.016	-0.455	0.394	0.59	π
$^3\Sigma_u^+$	-1	1_g	1.217	-0.516	0.557	0.86	π
$^3\Sigma_u^+$	0	0_g^-	1.538	-0.333	0.500	0.75	π
$^3\Sigma_u^+$	1	1_g	1.217	-0.516	0.557	0.86	π

We use the nine values of Ω_{mol} to calculate the total ionization rate constant. The rate constant for each of the nine contributions is calculated using the two-state model. The total ionization rate constant is obtained by summing over the nine contributions and weighing each contribution with a statistical factor of 1/9, where each rate constant is multiplied by its own Penning ionization probability p.

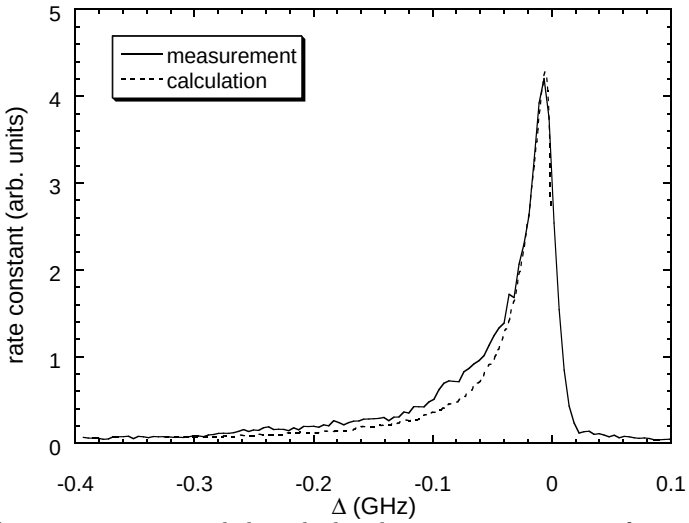

FIG. 5. The scaled measured ionization curve and the calculated ionization curve as a function of the detuning of the probe laser. The ion rate constant is expressed in arbitrary units.

The result of such a calculation, averaged over the thermal velocity distribution, corresponding to a temperature of 1 mK, is shown in Fig. 5. In the calculation we take into account that only a third of the light has the π- polarization required to make the transitions shown in Tab. I. Since for the measured curve neither a reliable absolute calibration was possible, nor a reliable determination of the background, we adapted the measured curve to the calculated one by choosing the background and the normalization to obtain best agreement. Therefore the comparison between the measurement and the calculation yields only information on the accuracy of the predicted shape of the curve. In Fig. 5 we can see that the shape of the ionization rate constant is very accurately predicted by the calculation. The slightly higher values in certain detuning ranges can be attributed to the photoassociation resonances discussed by Herschbach *et al.* [16]. The excitation of these bound states is not included in the semi-classical two-state model, so we expect to see these deviations. Therefore we can state that there is agreement within experimental error. This is a remarkable result considering the complexity of the system and the simplification that we made.

V. COMPARISON OF CALCULATED AND MEASURED ABSOLUTE IONIZATION RATE CONSTANTS

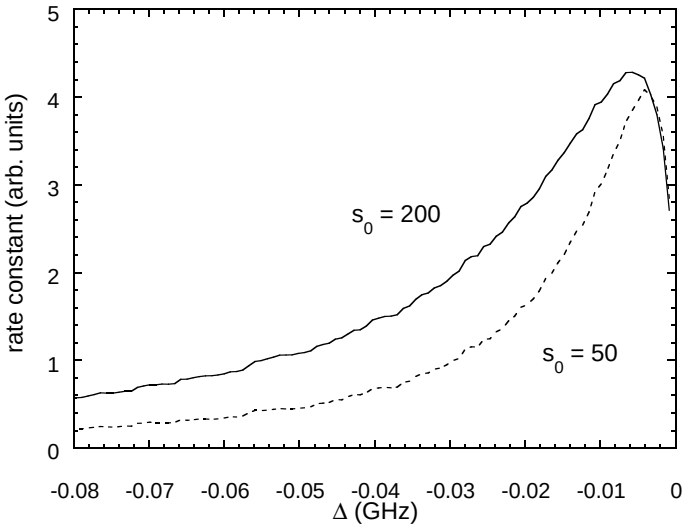

FIG. 6. Ionization rate constant calculated for $s_0 = 50$ (dashed line) and $s_0 = 200$ (solid line).

Since the agreement of the calculated behavior of the ionization rate constant with the measured behavior is so good, we are confident that the calculated absolute ionization rate constant should also be reasonably accurate. This is especially interesting, because existing experimentally determined absolute ionization rates are uncertain by factors of 2 to 100 [4–8]. In this section we will compare our calculated absolute ionization rate constant with the experimental ionization rate constants. All of these values have been determined at the detuning where the ionization rate constant is maximal, but under different experimental circumstances. Especially, different laser intensities have been used and slightly different MOT conditions and correspondingly slightly different temperatures. Our model allows us to judge the possible influence of these different conditions. As an example, we show the ionization rate constant in Fig. 6 calculated at a temperature of 1 mK for different saturation parameters, namely $s_0 = 50$ and $s_0 = 200$. We notice that the maximum value of the ionization rate constant, K^{ion}_{max}, is rather insensitive to the varied parameter. Since the uncertainties of the available experimental values are much larger than the variation of the calculated maximum rate constant for different experimental conditions, it is not necessary to account for these differences. It is sufficient to compare the calculated K^{ion}_{max} with the maximum values reported in the literature.

To be able to compare the measured and calculated rate constants, we must take care to use identical definitions for the rate constant. Therefore it is necessary to briefly outline the procedures that have been applied to obtain experimental ionization rate constants for optical collisions. In most experiments the ionization rate constant K^{ion} or the collision rate constant K was obtained from a measurement of the decay rate β of the MOT, when stopping the loading of the MOT. Note, that the collision rate constant K is a measure for all collisions resulting in trap loss, while the ionization rate constant K^{ion} only takes into account the collisions where an ion is formed. The ion rate or fluorescence rate is used to monitor the decrease of the density n. The valid assumption is made, that the decay is mainly due to collisions between trapped atoms. Hence a loss rate constant β is defined by $\mathrm{d}n/\mathrm{d}t = -\beta n^2$, where $\beta = 2K$. The factor 2 stems from the fact, that in one trap loss collision two atoms escape from the trap. We use the same definition in the semi-classical two-state model, *i.e.* $\mathrm{d}n_{ion}/\mathrm{d}t = Kn^2$, where n_{ion} is the ion density.

In order to experimentally determine the value of K, one needs to know n on an absolute scale. This poses severe problems and is the reason for the rather large uncertainties of the experimentally determined rate constants. Furthermore, some confusion has arisen because the experimentally determined rate constants have not been defined in the consistent way described above. Instead, one has argued that the ionization rate constant should be defined as the rate constant for ionization in collisions of excited $2^3\mathrm{P}_2$ atoms with ground state $2^3\mathrm{S}_1$ atoms. Hence the decay is given by $\mathrm{d}n_{ion}/\mathrm{d}t = 2K' n_p n_s = 2K'\pi_p(1-\pi_p)n^2$, where π_p is the population of the excited state [5]. The factor of 2 comes from the fact that we cannot distinguish between a collision of a S with a P atom and a P with a S atom. The rate constant at the detuning where the ion rate constant is maximal, K'_{max} is then found by assuming that the ensemble is saturated, *i.e.* that $\pi_p = 1/2$. For a given measured ion rate constant this leads to the relation $K'_{max} = 2K_{max}$, where K_{max} is our maximum rate constant.

TABLE II. Comparison of experimental values of K_{max} and K_{max}^{ion} with the theoretical value predicted by our two-state model and with each other. The corrected values are based on the definitions given in the text.

Reference	Published β_{max} (cm^3/s)	Corrected K_{max} (cm^3/s)	Published K_{max}^{ion}, (cm^3/s)	Corrected K_{max}^{ion} (cm^3/s)
Bardou *et al.* [5]	7×10^{-8} uncertainty: factor 4	3.4×10^{-8}	-	-
Tol *et al.* [6]	$(1.3 \pm 0.3) \times 10^{-8}$	$(6.5 \pm 0.3) \times 10^{-9}$	-	-
Browaeys *et al.* [8]	3×10^{-8} uncertainty: factor 2	1.5×10^{-8}	-	-
Kumakura *et al.* [7]	-	-	$(8.3 \pm 2.5) \times 10^{-8}$	$(2.1 \pm 0.6) \times 10^{-8}$
Mastwijk *et al.* [4]	-	-	$(1.9 \pm 0.8) \times 10^{-9}$	$(1.3 \pm 0.6) \times 10^{-9}$
This work	-	-	-	2.5×10^{-8}

This definition of K'_{max} is unphysical, which can be seen as follows. The rate constant is the product of the collision velocity and the cross section for ionization. This cross section is limited by the number of partial waves that can contribute. For $\Delta \gg \Gamma$, π_p goes to zero, while K still has a value of the order of K_{max}, as can be seen in Fig. 5. In that case the definition $\mathrm{d}n_{ion}/\mathrm{d}t = 2K'\pi_p\,(1-\pi_p)\,n^2$ would lead to unphysically large values of K', which would require ionization cross sections exceeding the maximum cross section, given the total number of partial waves. In Tab. II an overview is given of the measured values of β and K^{ion}_{max}' that are found in the literature. These values have been corrected to agree with our definition of K_{max} as defined above. In some of the experiments the collision rate constant K_{max} is determined and in other experiments the ionization rate constant K^{ion}_{max} is determined. Since we cannot estimate for each experiment the fraction of collisions that do lead to losses from the trap, but do not lead to ionization, we cannot compare every value with the calculation.

We notice that the experimentally determined ionization rate constant of Kumakura *et al.* [7] agrees within given limits of error with the value predicted by our calculation. However, the value of Mastwijk *et al.* [4] does not agree with the calculated ionization rate, which is due to an error made in determining the transmission through the mass spectrometer used to measure the ion rate. It is difficult to estimate the accuracy of the calculated value, as a result of the approximations that have been made. However, the K^{ion}_{max} is virtually independent of the experimental conditions used in the experiment. We therefore estimate that if our assumptions are correct, the calculated cross section is accurate to within 20%. We cannot calculate the collision loss rate K_{max} from K^{ion}_{max}, but it is clear that the K^{ion}_{max} should be a fraction of K_{max}.

VI. CONCLUSION

We have developed a semi-classical model to describe Penning ionization in optical collisions. The model is a two-state model, using a partial wave expansion and the Landau-Zener approximation to calculate the excitation rate. The predicted ionization rate constant as a function of the detuning of the light agrees well with measurements that we have done. Furthermore we have calculated the absolute ionization rate constant and compared it with measured absolute rate coefficients that have appeared in the literature. We have calculated an absolute ionization rate constant $K_{max} = 2.5 \times 10^{-8}$ cm^3/s. If we use a consistent definition of K_{max} we find good agreement with most quoted experimentally determined values.

---

[1] H.J. Metcalf and P. van der Straten, *Laser Cooling and Trapping*, Springer-Verlag, New York (1999).
[2] J. Weiner, V.S. Bagnato, S. Zilio, and P.S. Julienne, Rev. Mod. Phys. **71**, 1 (1999).
[3] M. Walhout, U. Sterr, C. Orzel, M. Hoogerland, and S.L. Rolston, Phys. Rev. Lett. **74**, 506 (1995).
[4] H. C. Mastwijk, J. W. Thomsen, P. van der Straten, and A. Niehaus, Phys. Rev. Lett. **80**, 5516 (1998).
[5] F. Bardou, O. Emile, J.-M. Courty, C.I. Westbrook, A. Aspect, Europhys. Lett. **20**, 681 (1992).
[6] P. J. J. Tol, N. Herschbach, E. A. Hessels, W. Hogervorst, and W. Vassen, Phys. Rev. A **60**, R761 (1999).
[7] M. Kumakura, and N. Morita, Phys. Rev. Lett. **82**, 2848 (1999).
[8] A. Browaeys, J. Poupard, A. Robert, S. Nowak, W. Rooijakkers, E. Arimondo, L. Marcassa, D. Boiron, C. Westbrook, and A. Aspect, Eur.Phys.J.D **8**, 199 (2000).
[9] A. Gallagher and D.E. Pritchard, Phys. Rev. Lett. **63**, 957 (1989)
[10] P.S. Julienne and J. Vigué, Phys. Rev. A **44**, 4464 (1991).
[11] K.-A. Suominen, J. Phys. B **29**, 5981 (1996)
[12] G. Woestenenk, H.C. Mastwijk, J.W. Thomsen, P. van der Straten, M. Pieksma, M. van Rijnbach, and A. Niehaus, Nucl. Instr. Meth. B **154**, 194 (1999).
[13] P.S. Julienne, A.M. Smith, and K. Burnett, Adv. At. Mol. Opt. Phys. **30**, 141 (1992).
[14] M. Movre and G. Pichler, J. Phys. B **10**, 2631 (1977).
[15] M. Müller, A. Merz, M.W. Ruf, H. Hotop, W. Meyer, and M. Movre, Z. Phys. D **21**, 89 (1991)
[16] N. Herschbach. P.J.J. Tol, W. Vassen, and W. Hogervorst, G. Woestenenk, J.W. Thomsen, P. van der Straten, and A. Niehaus, Phys. Rev. Lett. **84**, 1874 (2000)